

# A Well-Confined Redox Route to Silver Nanoparticles on the Surface of MoO<sub>3</sub>

Wenjun Dong, Shouhua Feng,\* Zhan Shi,  
Liansheng Li, and Yuehua Xu

State Key Laboratory of Inorganic Synthesis  
and Preparative Chemistry,  
College of Chemistry, Jilin University,  
Changchun 130023, People's Republic of China

Received December 13, 2002

Revised Manuscript Received March 31, 2003

The preparation of nanomaterials is a great challenge in the fields of synthetic chemistry and materials science because of the unusual properties that differentiate them from the bulk.<sup>1–13</sup> To utilize and optimize the chemical/physical properties of nanoscale metals, a number of workers have focused on the control of the size and/or shape of nanoparticles as well as their self-assembly into ordered structures by developing effective synthetic techniques. Several techniques, such as gas condensation,<sup>14</sup> irradiation,<sup>15,16</sup> sol–gel,<sup>17,18</sup> sonochemical deposition,<sup>19</sup> and nanostructured templates<sup>20–22</sup> for preventing the nanoparticles from irreversible aggregation, have been reported. Here, we report an effective well-confined redox method to prepare high-quality Ag nanoparticles. Our strategy was based on a self-redox

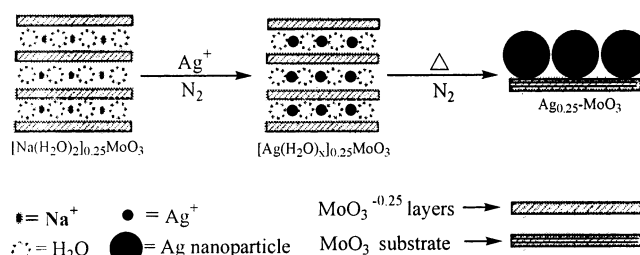


**Figure 1.** Formation of silver nanoparticles on the surface of the MoO<sub>3</sub> substrate. (Interlayer spacing of [Na(H<sub>2</sub>O)<sub>2</sub>]<sub>0.25</sub>MoO<sub>3</sub>,  $d_{020} = 9.72$  Å, and of [Ag(H<sub>2</sub>O)<sub>x</sub>]<sub>0.25</sub>MoO<sub>3</sub> ( $x = 1.5$ ),  $d_{020} = 9.41$  Å, and the size range of Ag nanoparticles is 3–10 nm.)

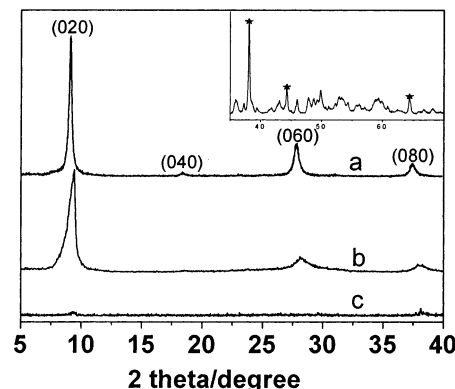
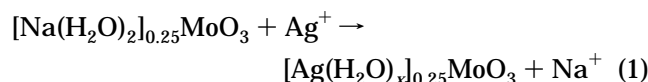


**Figure 2.** X-ray powder diffraction patterns for [Na(H<sub>2</sub>O)<sub>2</sub>]<sub>0.25</sub>MoO<sub>3</sub> (a), [Ag(H<sub>2</sub>O)<sub>x</sub>]<sub>0.25</sub>MoO<sub>3</sub> (b), and Ag<sub>0.25</sub>–MoO<sub>3</sub> treated at 330 °C for 10 min (c). Inset is also for Ag<sub>0.25</sub>–MoO<sub>3</sub> and the star-denoted peaks correspond to the cubic silver.

reaction that employed reductive [Na(H<sub>2</sub>O)<sub>2</sub>]<sub>0.25</sub>MoO<sub>3</sub> bronze and oxidative ion-exchanged silver ions. This in situ redox, at certain temperatures, led to the formation of Ag nanoparticles with tunable size.

The synthesis of [Na(H<sub>2</sub>O)<sub>2</sub>]<sub>0.25</sub>MoO<sub>3</sub> bronze was carried out according to a previously reported method.<sup>23</sup> The reaction of ion exchange of Na<sup>+</sup> by Ag<sup>+</sup> was first carried out in solution and then the self-redox reaction of [Ag(H<sub>2</sub>O)<sub>x</sub>]<sub>0.25</sub>MoO<sub>3</sub> at 330 °C in N<sub>2</sub> followed. The schematic reactions 1 and 2 are illustrated in Figure 1.



The identification of [Ag(H<sub>2</sub>O)<sub>x</sub>]<sub>0.25</sub>MoO<sub>3</sub> was carried out by X-ray powder diffraction (XRD). Typical layered structures of [Na(H<sub>2</sub>O)<sub>2</sub>]<sub>0.25</sub>MoO<sub>3</sub> (Figure 2a) and [Ag(H<sub>2</sub>O)<sub>x</sub>]<sub>0.25</sub>MoO<sub>3</sub> (Figure 2b) showed similar diffractions and the difference in their structures was only due to the sizes of the hydrated ions within the layers as the  $d$  spacing in the 0/0 direction was modified. Since the hydrated ionic radius of Ag<sup>+</sup> ion is smaller than that of Na<sup>+</sup>, the interlayer space of [Ag(H<sub>2</sub>O)<sub>x</sub>]<sub>0.25</sub>MoO<sub>3</sub> becomes smaller than that of [Na(H<sub>2</sub>O)<sub>2</sub>]<sub>0.25</sub>MoO<sub>3</sub>. The diffraction

\* Corresponding author. Fax: +86-431-5671974. Tel: +86-431-8499952. E-mail: shfeng@mail.jlu.edu.cn.

- (1) Interrante, L. V.; Hampden-Smith, M. J. *Chemistry of Advanced Materials*; Wiley-VCH: New York, 1998; p 271.
- (2) Schmid, G. In *Nanoscale Materials in Chemistry*; Klabunde, K. J., Ed.; Wiley-Interscience: New York, 2001; p 15.
- (3) Li, Y.; Liu, J.; Wang, Y.; Wang, Z. *Chem. Mater.* **2001**, *13*, 1008.
- (4) Hanamura, E. *Phys. Rev. B* **1988**, *37*, 1273.
- (5) Brune, H.; Romanczyk, C.; Roder, H.; Kern, K. *Nature* **1994**, *369*, 469.
- (6) Hyeon, T.; Fang, M.; Suslick, K. S. *J. Am. Chem. Soc.* **1996**, *118*, 5492.
- (7) Gibson, C. P.; Putzer, K. J. *Science* **1995**, *267*, 1338.
- (8) Ahmadi, T. S.; Wang, Z.; Green, T. C.; Henglein, A.; El-Sayed, M. A. *Science* **1996**, *272*, 1924.
- (9) Bromann, K.; Felix, C.; Brune, H.; Harbich, W.; Monot, R.; Buttet, J.; Lern, K. *Science* **1996**, *274*, 956.
- (10) Musick, M. D.; Keating, C. D.; Keefe, M. H.; Natan, M. J. *Chem. Mater.* **1997**, *9*, 1499.
- (11) Schmid, G. *Chem. Rev.* **1992**, *92*, 1709.
- (12) Petit, C.; Taleb, A.; Pileni, M.-P. *Adv. Mater.* **1998**, *10*, 259.
- (13) Shah, P. S.; Holmes, J. D.; Doty, R. C.; Johnson, K. P.; Korgel, B. A. *J. Am. Chem. Soc.* **2000**, *122*, 4245.
- (14) Hayashi, T.; Ohno, T.; Yatsuya, S.; Uyeda, R. *J. Appl. Phys.* **1977**, *16*, 705.
- (15) Mafuné, F.; Kohno, J.; Takeda, Y.; Kondow, T. *J. Phys. Chem. B* **2000**, *104*, 8333.
- (16) Abid, J. P.; Wark, A. W.; Brevet, P. F.; Girault, H. H. *Chem. Commun.* **2002**, 792.
- (17) Brugger, P. A.; Guendet, P.; Grätzel, M. *J. Am. Chem. Soc.* **1981**, *103*, 2923.
- (18) Shibata, S.; Aoki, K.; Yano, T.; Yamane, M. *J. Sol.-Gel Sci. Technol.* **1998**, *11*, 279.
- (19) Pol, V. G.; Srivastava, D. N.; Palchik, O.; Palchik, V.; Slifkin, M. A.; Weiss, A. M.; Gedanken, A. *Langmuir* **2002**, *18*, 3352.
- (20) Wang, T. C.; Rubner, M. F.; Cohen, R. E. *Langmuir* **2002**, *18*, 3370.
- (21) Sun, S.; Anders, S.; Hamann, H. F.; Thiele, J.-U.; Baglin, J. E.; Thomson, T.; Fullerton, E. E.; Murray, C. B.; Terris, B. D. *J. Am. Chem. Soc.* **2002**, *124*, 2884.
- (22) Dai, J.; Bruening, M. L. *Nano Lett.* **2002**, *2*, 497.

(23) Thomas, D. M.; McCarron, E. M., III. *Mater. Res. Bull.* **1986**, *21*, 945.

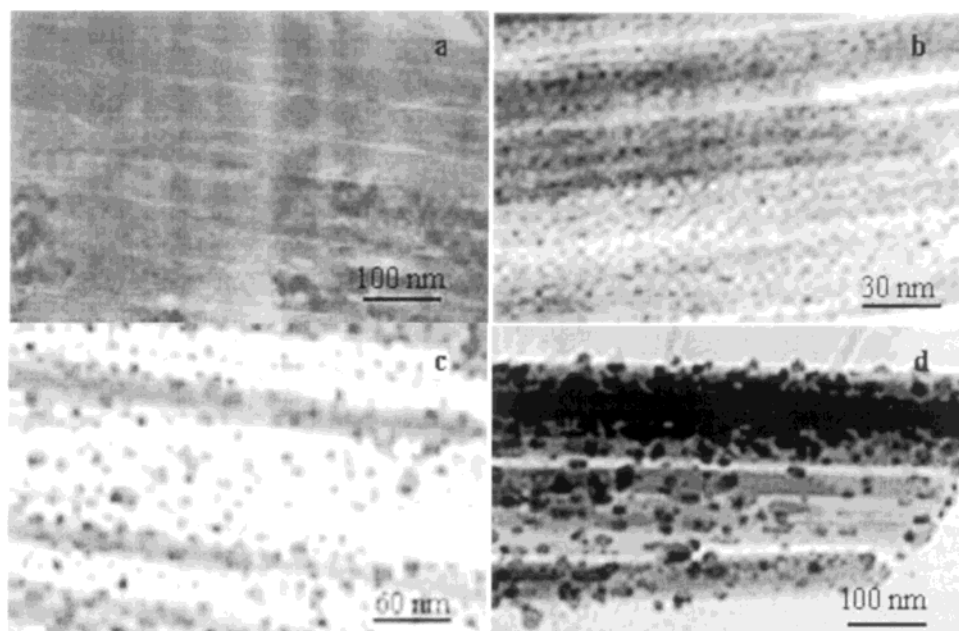


**Figure 3.** TEM images of layered  $[\text{Na}(\text{H}_2\text{O})_2]_{0.25}\text{MoO}_3$  (a); Ag nanoparticles on  $\text{MoO}_3$  substrate formed at  $330^\circ\text{C}$  for 10 min, particle size =  $3 \pm 0.5$  nm (b); 30 min, particle size =  $5 \pm 1$  nm (c) and 60 min, particle size =  $10 \pm 5$  nm (d).

of  $\text{Ag}_{0.25}\text{-MoO}_3$  (Figure 2c) indicates the formation of the cubic structure of Ag by its characteristic peaks (insert XRD pattern) and that of the disordered and exfoliated layers of  $\text{MoO}_3$ .

To confirm that the redox reaction had occurred, X-ray photoelectron spectroscopy (XPS) was used to identify the change in oxidation states for Mo and Ag atoms before and after the reaction. In the XPS spectra of Mo in the product ( $\text{Ag}_{0.25}\text{-MoO}_3$ ) and the starting material ( $[\text{Na}(\text{H}_2\text{O})_2]_{0.25}\text{MoO}_3$ ), a peak shift of 1.4 eV of Mo  $2\text{P}_{5/2}$  from lower (234.6 eV) to higher binding energies (236.0 eV) clearly indicated oxidation from  $\text{Mo}^{5.75+}$  to  $\text{Mo}^{6+}$ .<sup>24</sup> The XPS spectra of Ag  $2\text{P}_{3/2}$  in  $[\text{Ag}(\text{H}_2\text{O})_x]_{0.25}\text{MoO}_3$  and  $\text{Ag}_{0.25}\text{-MoO}_3$  showed a reduction from  $\text{Ag}^+$  to  $\text{Ag}^0$ , by indicating an energy shift from 368.5 eV ( $\text{Ag}^+$ ) to 367.9 eV ( $\text{Ag}^0$ ). The Ag  $3\text{d}_{5/2}$  peak at a binding energy of 367.9 eV with its fwhm of 1.9 eV showed a splitting of the 3d doublet of ca. 6.0 eV. All experimental values compare well with the reference values for  $\text{Ag}^0$  and  $\text{MoO}_3$ .<sup>24,25</sup>

The morphology and size distribution of Ag nanoparticles were observed on a Hitachi-8100IV transition electronic microscope (TEM). Figure 3a shows the typical layered structure of the starting material,  $[\text{Na}(\text{H}_2\text{O})_2]_{0.25}\text{MoO}_3$ . Figure 3b shows the Ag nanoparticle morphology of a sample obtained at  $330^\circ\text{C}$  after a 10-min heating treatment in which Ag nanoparticles were formed on the surface of the  $\text{MoO}_3$  substrate. TEM imaging showed the spherical Ag nanoparticles ca. 3 nm in diameter and with a narrow particle size distribution. Additionally, the particles were inhibited from gradual aggregation and dispersed on the surface of the  $\text{MoO}_3$  substrate. Due to the thermodynamic aggregation, the average size of the Ag particles increased with an increase in the heating time. For example, Ag particles with an average size of ca. 6 nm were obtained after a 30-min heating treatment (Figure 3c), while ca. 10-nm

Ag particles were obtained by further extending the reaction time to 60 min (Figure 3d). The structure of the  $\text{MoO}_3$  substrate became disordered as the Ag particles formed on the surface of the  $\text{MoO}_3$  substrate at relatively low temperatures such as  $300^\circ\text{C}$ , whereas the pure  $\text{MoO}_3$  is stable up to  $400^\circ\text{C}$ . Accordingly, in the initial stage of the redox reaction, the formed Ag atoms must be transferred from the interlayers onto the surface of the  $\text{MoO}_3$ , on which they were further aggregated into nanoparticles.

The thermal gravimetric and differential thermal analysis (TG-DTA) obtained in nitrogen gas provided additional evidence for the relationship between the redox reaction and structural stability. As expected, the TG-DTA of  $[\text{Na}(\text{H}_2\text{O})_2]_{0.25}\text{MoO}_3$  showed two stages of weight loss with distinct endothermic peaks at 100 and  $240^\circ\text{C}$ , which were assigned to the dehydration on the external surface and the interlayer. The TG-DTA curves of  $[\text{Ag}(\text{H}_2\text{O})_x]_{0.25}\text{MoO}_3$  can be divided into three corresponding stages: in the first stage, the endotherm accompanied by two steps of weight loss occurred at 100 and  $240^\circ\text{C}$ , which is attributed to dehydration; in the second stage, the exotherm in the range of  $300\text{--}330^\circ\text{C}$  is attributed to the self-redox reaction:  $\text{Ag}^+ + \text{MoO}_3^{0.25-} \rightarrow \text{Ag}_{0.25}\text{-MoO}_3$ ; in the third stage, an endotherm at ca.  $500^\circ\text{C}$  is due to the melting of the Ag nanoparticles. Moreover, when TG-DTA was carried out in the air, an endotherm at ca.  $500^\circ\text{C}$  with a weight gain of 1% was observed, due to the oxidation of the Ag nanoparticles, in accordance with the calculated value of 1.1%.

A UV-vis absorption spectral peak at 345 nm for 3-nm  $\text{Ag}_{0.25}\text{-MoO}_3$  was observed. It is attributed to the surface plasmon absorption of the silver clusters.<sup>26-28</sup> The electronic energy levels and optical transitions in the silver surface were extensively studied and it was confirmed that the transition from 4d to 5sp generally

(24) Briggs, D.; Seah, M. P., Eds.; *Practical Surface Analysis*; John Wiley and Sons: New York, 1983.

(25) Johnson, S. R.; Evans, S. D.; Mahon, S. W.; Ulman, A. *Langmuir* **1997**, *13*, 51.

(26) Esumi, K.; Suzuki, A.; Aihara, N.; Usui, K.; Torigoe, K. *Langmuir* **1998**, *14*, 3157.

(27) Kreibitz, U. *J. Phys. F: Met. Phys.* **1974**, *4*, 999.

(28) Henglein, A. *J. Phys. Chem.* **1993**, *97*, 5457.

occurred at around 320 nm.<sup>27,28</sup> The absorption of our well-dispersed Ag nanoparticles supported the formation of “quantum-dots”.<sup>29</sup>

In summary, we have demonstrated that Ag nanoparticles with controlled size could be fabricated based on multilayer MoO<sub>3</sub>. The flexibility of the silver ion exchange and the well-confined redox reaction greatly facilitate the fabrication of Ag nanoparticles on the surface of MoO<sub>3</sub>. Moreover, this well-confined prepara-

tion route for silver nanoparticles can be readily generalized to other systems.

**Acknowledgment.** This work was supported by the National Nature Science Foundation of China.

**Supporting Information Available:** Experimental details, XPS spectra, TG-DTA, and UV-vis spectra (PDF). This material is available free of charge via the Internet at <http://pubs.acs.org>.

CM0257825

---

(29) Beaglehole, D.; Hunderi, O. *Phys. Rev. B* **1970**, 2, 309.